

Федеральное государственное автономное образовательное
учреждение высшего образования « Московский физико-технический
институт (национальный исследовательский университе) »
Физтех-школа Электроники, Фотоники и Молекулярной Физики

На правах рукописи

Бейранванд Бехрох

Бехрох Бейранванд

**Разработка Массивов Оптических и
Терагерцовых Детекторов на Основе
Метаматериалов**

01.04.04 – « Физическая электроника »

АВТОРЕФЕРАТ

**Диссертации на соискание ученой степени
кандидата технических наук**

Научный руководитель:

к.ф.-м.н. Соболев Александр
Сергеевич

Москва 2020

Работа прошла апробацию на кафедре вакуумной электроники Федерального государственного автономного образовательного учреждения высшего образования «Московский физико-технический институт (национальный исследовательский университет)»

Научный руководитель: **Соболев Александр Сергеевич**

Ведущая организация:

Защита состоится «_» _____ г. в __ часов на заседании диссертационного совета _____ по адресу 141701, Московская область, г. Долгопрудный, Институтский переулок, д. 9. С диссертацией можно ознакомиться в библиотеке и на сайте Московского Физико-Технического Института (национального исследовательского университета) <https://mipt.ru/education/post-graduate/soiskateli-tekhnicheskie-nauki.php>

Работа представлена 2020 г. в Аттестационную комиссию федерального государственного автономного образовательного учреждения высшего образования «Московский физико-технический институт (национального исследовательского университета)» для рассмотрения советом по защите диссертаций на соискание ученой степени кандидата наук, доктора наук в соответствии с п.3.1 ст. 4 Федерального закона «О науке и государственной научно-технической политике».

Moscow Institute of Physics and Technology

Manuscript

Behrokh Beiranvand

Behrokh Beiranvand

**Development of Metamaterial-Based Optical and
Terahertz Detector Arrays**

Specialty 01.04.04 – « Physical electronics »

Synopsis

dissertation for the degree of
candidate of technical sciences

Supervisor: Alexander Sergeevich Sobolev

Moscow 2020

The work has been performed at the Department of Vacuum Electronics Federal State Autonomous Educational Institution of Higher Education «Moscow Institute of Physics and Technology(National Research University)» Phystech School of Electronics, Photonics and Molecular Physics.

Supervisor: Alexander Sergeevich Sobolev

The defense of the dissertation will be held on " _ " _____ at __ , at the meeting of the dissertation council _____. _____, at 141701, Moscow region, Dolgoprudniy, Institutskiy per., 9, MIPT. The dissertation is stored in the library and published on the site of Moscow Institute of Physics and Technology (national research university). <https://mipt.ru/education/post-graduate/soiskateli-tekhnicheskie-nauki.php>

The work was submitted on _____ to the Attestation Commission of the Moscow Institute of Physics and Technology (National Research University) for consideration by the council for the defense of dissertations for the degree of candidate of science, doctor of science in accordance with paragraph 3.1 Art. 4 of the Federal Law «On Science and State scientific and technical policy».

General description of the subject of work

The dissertation is devoted to the development of Metamaterial (MTM) for detection at optical and terahertz frequencies. This work presents research and design of MTMs in two parts, first section describes the cold electron bolometers (CEBs) which have been introduced and invented by L. S. Kuzmin and in second section, optical and terahertz MTMs are discussed.

In the first section we attempted to investigate various designs of CEBs based on superconductor-insulator-normal metal-insulator-superconductor (SINIS) tunnel junctions with array structures. Here, the selected motifs of array structures are annular and meander patterns from the frequency selective surface (FSS) and act as detector for incident wave radiations. The operations of CEB devices such as designing and studying these arrays in a wideband for the range 300-450 GHz and ultrawideband for the range 200-1000 GHz, a model of dual band cold electron bolometer at 210 GHz and 240 GHz and other models to work in two modes of polarization are reported. In the abovementioned CEB designs, first large-size UC¹ for balloon-borne telescope missions are briefly noted and compared with the small-size UCs.

The second section a method is proposed for generating terahertz radiation using a array of thermocouples with capacitive coupling heated by femtosecond laser pulses. Here we present a model of composite right/left handed transmission line.

In the next part of this section we are going to report a numerical study of drag effect plasmonic MTM consisting of three layers SiO₂/ Au/ Si with the aim of absorption for 1 um laser in spectral regime for infrared operation and also provide an edge states plasmonic MTM consisting of four layers SiO₂/Ag/SiO₂/Si with the aim of molecules detection in visible spectral regime for near field Raman spectroscopy which operates by using the topological insulator. The results showed us that we are able to benefit the edge states at several different frequencies (pixels) for this nano-structure. The nano-structure was irradiated for the range of 500-650 THz. Also two proposals for dual-band plasmonic absorber are presented which geometrically and dynamically are tunable and can be used as optical detectors.

The goals of the thesis

¹ Mahashabde S. Frequency selective cold-electron bolometer arrays // Chalmers University of Technology. — 2015.

1. Theoretical development and optimization of the arrays of planar antennas of terahertz frequency range with integrated cold-electron bolometers based on SINIS nanostructures for radio astronomy research.
2. Design and numerical investigation of a hybrid type (left-right handed) transmission line consisting of a 1D array of thermocouples for microwave and terahertz radiation under excitation by femtosecond optical pulses.
3. Numerical investigation of local enhancement of the electric field in plasmonic crystals associated with existence of topological photonic edge states around the break of periodic symmetry.
4. Investigation the possibility of enhancement and tunability of optical absorption in plasmonic crystals containing graphene above the nanostructured metal layer. Present two tunable plasmonic absorbers based on a layer of graphene with two resonators and one resonator.

The tasks of the thesis

1. An ultrawideband design of a periodic 2D array of CEBs with subwavelength size of unit cell (UC) has been developed and studied. Numerical analysis has demonstrated that this array mounted on a silicon lens may absorb more than 70% of incident terahertz power in the frequency range from 200 GHz to 1 THz.
2. A dual-polarization layout of a sparse periodic array of CEBs with the UC size as much as half wavelength has been developed and optimized for the range 210-240 GHz. In both arrays the bolometers are connected in parallel for the incoming terahertz radiation, while at DC they are connected in series to add up the voltage responses.
3. A hybrid transmission line with anomalous dispersion and hyper-light phase velocity is proposed and numerically investigated. This line is based on the 1D array of thermocouples, which produce collective voltage response on a subpicosecond time scale upon illumination by a femtosecond laser light.
4. Up to 11 field enhancement of the local electric field has been discovered in plasmonic crystals patterned on Si/SiO₂/Ag/SiO₂ layered structure with defects in translational

symmetry. The effect of local field enhancement, which highest value is achieved at 550 THz, is associated with topological photonic states existing on the photonic crystal boundary. This effect can be employed for Raman spectroscopy and increasing Purcell factor of quantum dots.

5. Two types of a dual band tunable graphene-based plasmonic absorber has been proposed. The first one consists of periodical array of elliptical grooves in Ag film covered by SiO₂ and graphene layers. Absorption at two peaks around 1500 nm and 1700 nm can be tuned from 20% to 90% by rotation of the polarization plane of incident light and from 30% to 50% by applying gate voltage. The second absorber consists of a periodic array of concentric circular grooves in Ag film with SiO₂ and graphene layer on top of it. Absorption peaks at 1100 nm and 1700 nm can be tuned from 80% to 97% by applying gate voltage.

Scientific novelty

The aim was to create and study distributed structure for detection of terahertz and optical radiation. This structure (1D, 2D) consists periodically translated UC and we confine electrodynamic properties of this structure as if it was a homogenous material (for the lowest modes of the Floquet UC). Compared to previous works in the designs of CEBs, we developed several designs for increasing the bandwidth, being dual-band, and having the absorption of the UC relative to the different polarizations. In another part of this dissertation, an attempt was made to simulate a structure and a new theory was defined and mentions how it is possible to generate a terahertz wave using nonequilibrium states of an electron gas in metals. Thermocouples are combined in a hybrid transmission line with superluminal phase velocity for their mutual synchronization. In the plasmonic part of this dissertation, several new and fabricate-able structures are presented, which: 1) A simulated sample for the visible range is presented which can be used in red, green, etc pixels by edge state plasmonic topology, and 2) two tunable plasmonic absorbers were presented and in general, the advantages of the proposed structures over similar devices are first easily measurable response to physical rotation and polarization angle, and then providing two individually tunable absorption peaks.

The theoretical and practical value

The designs are numerically done in the framework of finite difference time-domain (FDTD) method so that they can be accurately concluded before fabrication. From the numerical and theoretical point of view, the structures can be used and flexible in changing the design so that theoretical and numerical tests can be performed at different frequencies. The samples presented in each section are according to the scientific and practical requirements in that field. If we want to refer to CEBs, we must say that scientists have been tended to study deep full-sky survey and the Cosmic Microwave Background hence it has led them to design cryogenic bolometers. Investigated CEBs in this dissertation to install on telescopes for OLIMPO missions are considered. The hybrid transmission line proposed in this dissertation adapts all responses in phase and can be used in high frequency and radio-optical applications. The plasmonic edge state design can be useful in various applications such as medical, drag sensors, raman spectroscopy, etc. The proposed multi-functional tunable dual-band plasmonic absorber can be used in several applications including magneto-optic modulation, rotation detection, electro-optic modulation and spectral selective tunable absorption. Finally the dual-band tunable plasmonic absorber using concentric-rings resonators and mono-layer graphene has practical applications such as tunable light absorber with fully controllable absorption spectrum that can be used in a wide range of applications from photo-detectors to multi spectral tunable reflectors.

Statements to be defended.

The statements to be defended in the thesis can be enumerated as follows:

1. Present a wideband 2D-array of periodically arranged electrically small rings, each containing Cold-Electron bolometers, which may potentially absorb 50 to 80 percent of the incident terahertz power with linear polarization. The array consists of a periodically arranged UCs each containing a ring with the four CEBs.
2. Two arrays of CEBs with respect to different modes of incident power. Here UCs are designed that can absorb acceptable amount of power in different modes.
3. A numerical study of dual-band CEB, which work at two frequencies about 210 GHz and 240 GHz. The array consists of a periodically arranged UCs each containing two rings with the eight bolometers. The purpose of this design is a simultaneous operation of the array structure at two different frequencies.

4. Present a novel type of a wideband 2D array of CEBs sensitive to both polarizations of the incoming optical signal. The array consists of a periodic sparse array of the orthogonal $\lambda/2$ dipoles and is centered at 330 GHz with more than 10% bandwidth for dual polarization and 25% bandwidth for a single polarization. An imaging pixel based on the proposed sparse array is the most promising for combination of high efficiency and low noise of the system and satisfying the 10% bandwidth requirements for OLIMPO telescope.
5. A concept of the thermoelectric structure that generates microwave and terahertz signals when illuminated by femtosecond optical pulses. The structure consists of a series array of capacitively coupled thermocouples. The array acts as a composite right/left handed microwave transmission line with anomalous dispersion and phase velocity higher than the velocity of light.
6. A numerical study of edge states plasmonic metamaterial consisting of four layers $\text{SiO}_2/\text{Ag}/\text{SiO}_2/\text{Si}$. The proposed structure can obtain reasonable results in response to a frequency detection of the green laser range. Metamaterial is examined for two modes of radiation and with changes in the angle of excitation, the acceptable responses are observed at several frequencies from other visible frequency bands.
7. Present two plasmonic absorbers which show a highly absorptive behavior at near infrared wavelengths due to the strong confinement of the electromagnetic field inside the grooves of the metal layers. Simulation results show that, modulation of absorption per graphene Fermi energy, about 73.33 %/eV and 69.54 %/eV for absorber with one resonator and can be achieved for the first and the second peaks, respectively. And for absorber with two resonators tunability factors (modulation of absorption per graphene Fermi energy) of 85 %/eV and 51.25 %/eV are calculated for the first and the second peaks, respectively.

Presentations and validation of research results.

The results of the thesis were published in IEEE Transactions on Antenna and Propagation (Q1, WoS), Journal of Optics (Q1, WoS), Optik (Q2, WoS) and reported and discussed at the following scientific conferences and seminars:

1. 60th Scientific Conference MIPT. Moscow, Russia. 2017.
2. Proceedings of the VI All-Russian Microwave Conference. Moscow, Russia. 2018.

3. Radiation and Scattering of Electromagnetic Waves RSEMW. Divnomorskoe, Russia. 2019.
4. International Congress on Graphene, 2D Materials and Applications. Sochi, Russia. 2019.

List of publications

1. [Web of science and Scopus, Q1] Beiranvand B., Sobolev A. S. A proposal for a multi-functional tunable dual-band plasmonic absorber consisting of a periodic array of elliptical groove// Journal of optics. —2020. —V. 22, № 10. —P. 105005. DOI: <https://doi.org/10.1088/2040-8986/abb2f3>
2. [Scopus] Sobolev A. S., Kuzmin L. S., Beiranvand B., Kudryashov A. V., Ilin A. Ultrawideband Metamaterial-Based Array of Cold-Electron Bolometers// Radiation and Scattering of Electromagnetic Waves (IEEE). —2019. —P. 196-199. DOI: [10.1109/RSEMW.2019.8792785](https://doi.org/10.1109/RSEMW.2019.8792785)
3. [Scopus] Sobolev A. S., Beiranvand B., Chekushkin A. M., Kudryashov A. V., Tarasov M. A., Yusupov R. A., Gunbina A., Vdovin V. F., Edelman V. Wideband metamaterial-based array of SINIS bolometers// European Physical Journal Web of Conferences (EDP Sciences).—2018.—V.195. —P. 05009. DOI: [10.1051/epjconf/201819505009](https://doi.org/10.1051/epjconf/201819505009)
4. [Web of science and Scopus, Q1] Kuzmin L. S., Sobolev A. S., Beiranvand B. Wideband Double-Polarized Array of Cold-Electron Bolometers for OLIMPO Balloon Telescope// Transactions on Antennas and Propagation (IEEE). —2020. DOI: [10.1109/TAP.2020.3026874](https://doi.org/10.1109/TAP.2020.3026874)
5. [Web of science and Scopus, Q2] Beiranvand B., Sobolev A. S., Sheikha A. A proposal for a dual-band tunable plasmonic absorber using concentric-rings resonators and mono-layer graphene// Optik International Journal for Light and Electron. —2020. —V. 223. —P. 165587. DOI: <https://doi.org/10.1016/j.ijleo.2020.165587>
6. Бейранванд Б., Соболев А. С. Гибридная линия передач с интегрированной цепочкой термопар для генерации терагерцового излучения// Труды 60-й Всероссийской научной конференции МФТИ. —2017. —с. 149-151.
7. Бейранванд Б., Вдовин В. Ф., Гунбина А. А., Ермаков А. Б., Лемзяков С. А., Мансфельд М. А., Махашабе С., Нагирная Д. В., Соболев А. С., Тарасов М. А., Фоминский М. Ю., Чекушкин А. М., Эдельман В. С., Юсупов Р. А., Якопов Г. В. Матрицы

планарных антенн с интегрированными СИНИС болометрами для радиоастрономических исследований// Сборник трудов VI Всероссийской микроволновой конференции. —2018. — с. 253-257.

8. Соболев А. С., Бейранванд Б., Тарасов М. А., Юсупов Р. А., Гунбина А. А., Чекушкин А. М., Эдельман В. С. Двухчастотная метаповерхность с интегрированными СИНИС болометрами// Сборник трудов VI Всероссийской микроволновой конференции. —2018. —с. 310.

9. [RCSI] Бейранванд Б., Соболев А. С., Кудряшов А. В. Гибридная линия передач с интегрированной цепочкой термопар для генерации терагерцового излучения // Труды МФТИ. —2020. —Т. 12, № 3. —с. 87–93.

Personal contribution

The main contributions of the author in the thesis can be summarized as follows:

The author in **(1)** and **(5)** proposed two new absorbers. In **(1)** a tunable plasmonic absorber composed of an elliptically grooved metallic film sandwiched between two dielectric layers was presented. It was shown that the proposed device can provide two absorption peaks, in the near-infrared region, with absorption coefficients dependent upon the polarization angle of the incident light. It was discussed that by adding a graphene layer to the structure, a tunable dual band modulator is realized, by which two absorption bands can be adjusted independently. Simulation results show that modulations of absorption per graphene Fermi energy, about 73.33% eV^{-1} and 69.54% eV^{-1} are achieved for the first and the second peaks, respectively². And in **(5)** a hybrid plasmonic absorber consisting of graphene and silica layers coated on a metal film with concentric-rings grooves was presented and numerically investigated. The proposed structure provides two absorption peaks at near-infrared region. The absorptivity of each peak can be tuned independently, by controlling the chemical potential of the graphene layer. Modulation of absorption per graphene Fermi energy about 85% eV^{-1} and 51.25% eV^{-1} can be obtained for the first and the second peaks, respectively³. Author in articles related to CEBs optimized topological parameters. So that in **(4)** an array of CEB was presented, which in two

² Beiranvand B., Sobolev A.S. A proposal for a multi-functional tunable dual-band plasmonic absorber consisting of a periodic array of elliptical groove// Journal of optics. —2020. —V. 22, № 10. —P. 105005.

³ Beiranvand B., Sobolev A.S., Shekhale A. A proposal for a dual-band tunable plasmonic absorber using concentric-rings resonators and mono-layer graphene// Optik International Journal for Light and Electron. —2020. . —V. 223. —P. 165587.

modes, in addition to optimizing NEP 4 times, the bandwidth also reached more than 10%, which can be installed for OLIMPO. In (2), (3) and (7), in addition to increasing the bandwidth by reducing the size of the UC, absorption for different modes with DC wire as well as the study of tangential components were concluded. In (8) a dual-band UC was simulated for x mode, capable of simultaneously absorbing two frequencies, 210 and 240 GHz. In (6) and (9) a concept was presented so that by arranging an array of thermocouples as a transmission line we could generate terahertz pulses with a pico-second laser. In general, the personal contribution of the author in the articles can be summarized as follows:

- Developing concepts of new electrodynamic systems based on periodic structures that are supposed to operate at terahertz and optical frequencies
- Creating numerical models of periodic structures and performing their numerical and theoretical studies of EM-properties at terahertz and optical frequencies.
- Making design and optimization of periodic structure layouts, creating CAD models for fabrication of planar periodic structures
- Creating diagrams and figures, writing the text of manuscripts

The structure and amount of the thesis

The thesis consists of an abstract, five chapters and list of 231 references. The full volume of the dissertation is 151 pages, including 77 figures and 3 tables.

The content of the work

The abstract presents a brief description of the whole dissertation that defines the purpose of each section. It is explained that the dissertation is divided into three sections, one section is related to CEBs, the next section is about generating terahertz pulses using a hybrid transmission line composed of thermocouples, and the last section is for designing several plasmonic structures.

The 1st chapter provides a complete overview of previous works on balometers and their comparison. The purposes of using balometers as well as CEB are also discussed. **The 2nd Chapter** deals with the performance of CEBs in more detail. Since this chapter describes the

CEB and this type of bolometer is a superconducting bolometer, first superconductivity is described in **2.1.1**, acting of absorber and then review the NIS that performs as the basic function. This chapter also includes the concept of SINIS junctions. Then it refers to some of the most influential processes in the theory, such as the noises and responsivity. As it is mentioned in **2.1.1** in 1911, superconductivity was introduced as a phenomenon⁴ and its properties was discussed in 1957⁵ that shows some metals reduce the electrical resistance to zero (there is no power loss) and creates a diamagnetism phenomenon when the temperature of the metal is lower than the critical temperature T_c . In the BCS theory, there is a gap which is shown by the parameter Δ and it is defined below the T_c temperature. In fact, it is the energy difference between the ground state of the superconductor and the energy of the lowest quasiparticle excitation^{6,7} and 2Δ is the minimum energy that is needed to break a pair. Based on the BCS theory at zero temperature

$$\Delta(T) = 1.76K_B T_c \quad (1)$$

here $T=0$ and K_B is the Boltzmann constant. As it is described in **2.1.2** between the superconducting state and the normal state there is a different in the quasiparticle density of states and the mentioned parameter Δ is the main factor to analyse the superconducting density of states. When the temperature of the superconductor is above T_c from BCS theory the superconducting density of states is⁸

$$D(E) = D(0) D_N \quad (2)$$

$$D_N = \left| \operatorname{real} \left(\frac{E}{\sqrt{E^2 - \Delta^2}} \right) \right| \quad (3)$$

where $D(0)$ is the two-spin density of states at the Fermi level and D_N is the normalized density of states when $T = 0$ K. If $E = \Delta$ there is no states below the gap. In **2.1.3** by explaining the hot electron effect and normal metal as an absorber, it is mentioned that the Fermi function is a function that shows the behavior and its temperature dependence. The distribution function of a metal (can be a normal metal or a superconductor) in equilibrium is⁹

⁴ Onnes H. K. Further experiments with liquid helium. C. on the change of electric resistance of pure metals at very low temperatures etc. IV. the resistance of pure mercury at helium temperatures// In Through measurement to knowledge. Springer. — 1991. — P. 261-263.

⁵ Bardeen J., Cooper L. N., Schrieffer J. R. Theory of superconductivity// Phys. Rev. — 1957. — V. 108. — P. 1175-1204.

⁶ Tinkham M. Introduction to superconductivity// Courier Corporation, 2004.

⁷ Timusk T. The superconducting energy gap// La Physique Au Canada. — 2011. — V. 67, № 2. — P. 99.

⁸ Dynes R., Narayanamurti V., Garno J. P. Direct measurement of quasiparticlelifetime broadening in a strong-coupled superconductor// Physical Review Letters. — 1978. — V. 41, № 21. — P. 1509.

⁹ Golubev D., Kuzmin L. S., Willander M. SIN tunnel junction as a temperature sensor// In Photodetectors: Materials and devices IV. — 1999. — V. 3629. — P. 364- 370.

$$f(E) = \frac{1}{e^{\frac{E}{k_B T_e}} + 1} \quad (4)$$

where T_e is the electron temperature and K_B is the Boltzmann constant. Since the time constant of the electron-phonon interaction is much larger than the time constant electron-electron an electron distribution with an increased effective temperature can be created. In a junction such as NIS the normal metal acts as an absorber and incident radiation increases the temperature of electrons which are called hot electrons. In 2.2 the NIS junction and tunneling are described. Figure 1 is illustrated the energy band diagram of the biased NIS junction. The Fermi of occupied states in the normal metal is above the gap of superconductor and electrons are moved by tunneling through the insulator from the normal metal to superconductor. The direction of the moving of electron and the direction of the current are shown. The small changes in bias will result in large changes in current. The number of the electrons which are participate in this process rapidly change with bias.

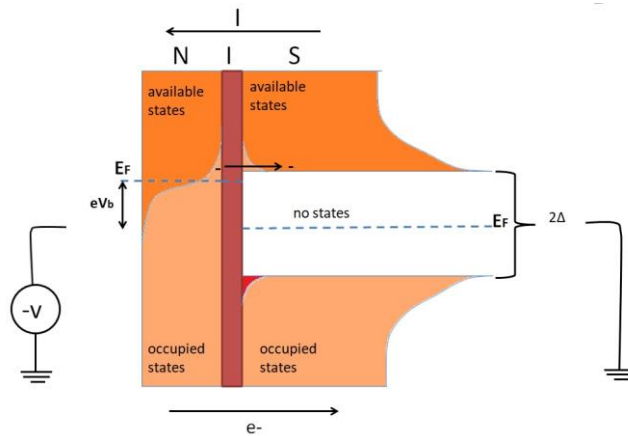


Figure 1 Energy band diagram of the biased NIS junction

According to 2.2.1 the NIS current is¹⁰:

$$I_{NIS} = e \int_{-\infty}^{+\infty} [\Gamma_{NS} - \Gamma_{SN}] dE = \frac{1}{eR_{NS}} \int_{-\infty}^{+\infty} D(E) (f_N(E - eV) - f_S(E)) dE \quad (5)$$

where $D(E)$ is density of states, R_{NS} is the normal state resistance and V is the voltage. So based on this equation the V-I characteristic and Power deposited in the absorber (normal metal) and superconductor (2.2.2) can be described.

¹⁰ O'Neil G. C. Improving NIS tunnel junction refrigerators: Modeling, materials, and traps// Santa Clara University. — 2011.

A schematic of the CEB with NIS junctions is provided in Figure 2. Incident power is supplied and dissipated in the normal metal absorber. The photon energy is absorbed by heating electrons in the absorber and this increasing of the temperature is measured by the NIS junctions. By this method, L. S. Kuzmin introduced another generation of bolometers as CEB. Heat balance equation (HBE)^{11,12}(2.3.1), Responsivity¹² (2.3.2) and Noise Equivalent Power (NEP)^{12,13 14,15,16}(2.3.3) for this junction are as follow:

$$2P_N + 2\beta P_S - \sum \Lambda(T_e^5 - T_{ph}^5) + P_j + P_0 + \partial P = 0 \quad (6)$$

$$S_I = 2 \frac{\left(\frac{\partial I}{\partial T}\right)}{5 \sum \Lambda T_e^4 + \left(\frac{\partial P}{\partial T}\right)} \quad (7)$$

$$S_V = -2 \frac{\left(\frac{\partial I}{\partial T}\right)}{\frac{\partial V}{\partial V}} \cdot \frac{1}{5 \sum \Lambda T_e^4 + 2\left(\frac{\partial P}{\partial T} - \frac{\partial I}{\partial T} \times \frac{\partial P}{\partial V}\right)} \quad (8)$$

$$NEP_{tot}^2 = NEP_{amp}^2 + 2 A NEP_{NIS}^2 + A NEP_{e-ph}^2 + A NEP_{ph}^2 \quad (9)$$

where equation (6) is HBE, equation (7) and (8) are current and voltage Responsivity and equation (9) is NEP. In equation (6) β is the fraction of power returning from the superconductor to the normal metal¹⁷, $\sum \Lambda(T_e^5 - T_{ph}^5)$ describes the heat flow from electron to the phonon subsystems in the normal metal absorber, \sum is material constant, Λ is the volume of the normal metal absorber, T_e and T_{ph} are temperature of the electron and phonon, respectively¹⁸; P_j is power of joule heating which is equal $I^2 R_{abs}$ where R_{abs} is the resistance of the absorber, P_0 and ∂P are the steady background power and the incident signal power, respectively. In equation (9) A is the number of CEB which is important parameter to adjust NEP_{tot} less than NEP_{phot} .

¹¹ Mahashabde S. Frequency selective cold-electron bolometer arrays // Chalmers University of Technology. — 2015.

¹² Golubev D., Kuzmin L. Nonequilibrium theory of a hot-electron bolometer with normal metal-insulator-superconductor tunnel junction// Journal of Applied Physics. — 2001. — V. 89, № 11. — P. 6464-6472.

¹³ Kuzmin L., Yassin G., Withington S., Grimes P. An antenna coupled coldelectron bolometer for high performance cosmology instruments// Proc. of the 18th ISSST. — 2007. — P. 93-99.

¹⁴ Richards P. Bolometers for infrared and millimeter waves// Journal of Applied Physics. — 1994. — V. 76, № 1. — P. 1-24

¹⁵ Kuzmin L. Ultimate cold-electron bolometer with strong electrothermal feedback// In Millimeter and submillimeter detectors for astronomy II. — 2004. — V. 5498. — P. 349-361.

¹⁶ Jethava N., Chervenak J., Brown A.-D., Benford D., Kletetschka G., Mikula V., Kongpop U., others. Development of superconducting transition edge sensors based on electron-phonon decoupling// In Millimeter, submillimeter, and far-infrared detectors and instrumentation for astronomy V. — 2010. — V. 7741. — P. 774120.

¹⁷ Fisher P., Ullom J., Nahum M. High-power on-chip microrefrigerator based on a normal-metal/insulator/superconductor tunnel junction// Applied physics letters. — 1999. — V. 74, № 18. — P. 2705-2707.

¹⁸ Kuzmin L. S., Perera A. Cold-electron bolometer. In Bolometers// INTECHWEB. ORG. — 2012. — P. 77-106.

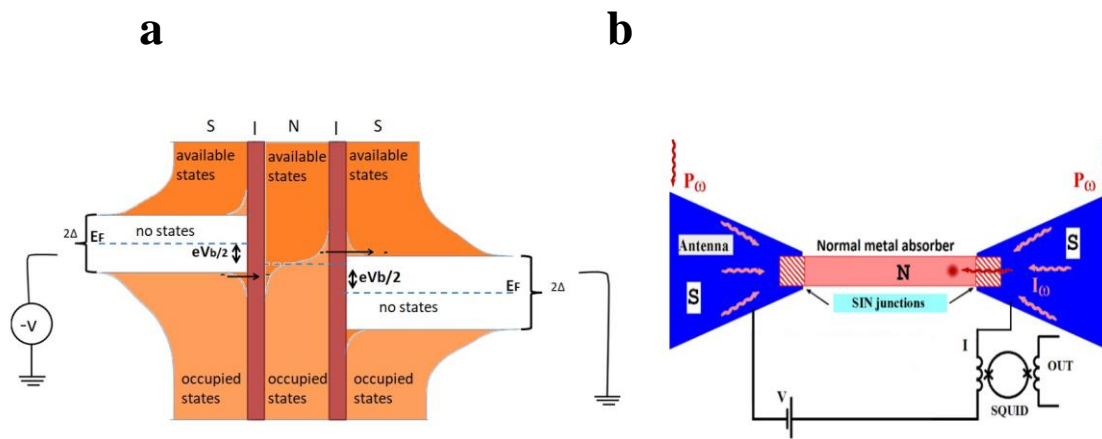


Figure 2 a) Energy diagram of the SINIS structure, b) Cold-Electron Bolometer (CEB) with NIS tunnel junctions by L. S. Kuzmin¹⁹

The 3rd chapter reviewing the Frequency Selective Surfaces in 3.1, points to two previously designed samples at Chalmers University (3.1.2) (3.1.3) and then in (3.2) Wideband FSS array based on CEB (Small size UC) is presented. In this subsection a wideband 2D-array of periodically arranged electrically small rings, each containing SINIS bolometers, which may potentially absorbs 50 to 80 percent of the incident terahertz power with linear polarization is developed and studied. The array consists of a periodically arranged UCs each containing a ring with the four CEBs. This design is shown in Figure 3. In 3.2.1 a UC (Figure 3) of the FSS in which the CEBs have been integrated is described. It is an annular pattern with extended lines as split-ring. The modeling was carried out by CST STUDIO SUITE software package. Earlier such bolometers were designed and studied numerically and experimentally as it is mentioned in (3.1.3), and demonstrated voltage responsivity up to 10^9 V/W with a bandwidth of 5-10% in a 350 GHz frequency band.

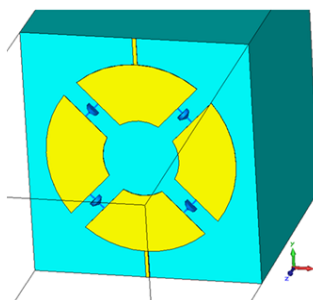


Figure 2 Design of UC in which blue arrows are simulated CEB

¹⁹ Kuzmin L., Yassin G., Withington S., Grimes P. An antenna coupled coldelectron bolometer for high performance cosmology instruments// Proc. of the 18th ISSTT. — 2007. — P. 93-99.

In the following, the method of defining impedances in **3.2.2**, the results for different polarizations in **3.2.3** and **3.2.4** are presented numerically. **3.2.5** is actually experimental measured.

3.3 describes FSS array based on CEB for dual mode design for arbitrary polarization. In **3.3** we aim to investigate the FSS+CEBs with respect to different modes of incident power. Here UCs are designed that can absorb an acceptable amount of power in different modes. In **3.2** a UC is produced that mode#2 could not see DC-biasing wires in **3.3** we are going to introduce a concept of FSS+CEBs which gives array to have absorptivity of two modes. The structures are presented in **3.3.1**. The investigated UCs are shown in Figure 3. The calculated absorbed powers based on these equations are achieved in **3.3.2**:

$$P_{\text{abs}} = |a|^2 \int_0^{\pi/2} \cos^2\theta d\theta + |a|^2 \int_0^{\pi/2} \sin^2\theta d\theta \quad (10)$$

$$P_{\text{abs}}^{\text{arb}} = \frac{P_{\text{abs}}^{(1)} + P_{\text{abs}}^{(2)}}{2} = |a|^2 \int_0^{\pi/2} \cos^2\theta d\theta + |a|^2 \int_0^{\pi/2} \sin^2\theta d\theta \quad (11)$$

3.4 present a numerical study of dual-band cold-electron bolometers (CEB), which work at two frequencies about 210 GHz and 240 GHz. The array consists of a periodically arranged UCs each containing two rings with the eight bolometers. The purpose of this design is a simultaneous operation of the array structure at two different frequencies. **3.4.1** describes the structure of the design and simulation results are in **3.4.2**.

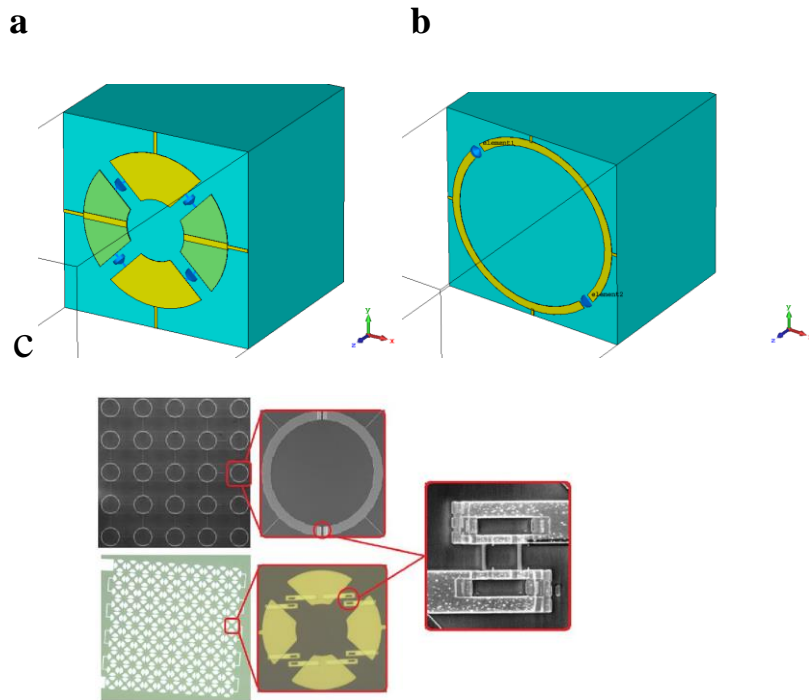


Figure 3 Dual mode UCs for arbitrary polarization a) with four CEBs, b) with two CEBs and c) photos of manufactured samples.

3.5 presents a novel type of a wideband 2D array of CEBs sensitive to both polarizations of the incoming optical signal is proposed. This array was developed for OLIMPO balloon telescope with requirement on bandwidth more than 10%. Sensitivity to both polarization components was achieved by special meander-type arrangement of orthogonal L/2 dipoles. A pixel layout with optimal density of CEBs, sensitive to dual polarizations and having more than 10% FWHM bandwidth at around 350 GHz was proposed and numerically analyzed. The layout consists of a periodic sparse array of an orthogonal dipoles sensitive to both polarization components of incoming signal. Numerical analysis confirmed that the sparse array is the most promising for combination of high absorbing efficiency and low noise of the system and satisfying the 10% bandwidth requirements for OLIMPO instrument. Different combinations of series and parallel connections of bolometers were considered for better noise properties to achieve the photon noise-limited level. NEP analysis in 3.5.1 shows that the optimized results of NEP as it can be seen in Figure 4.

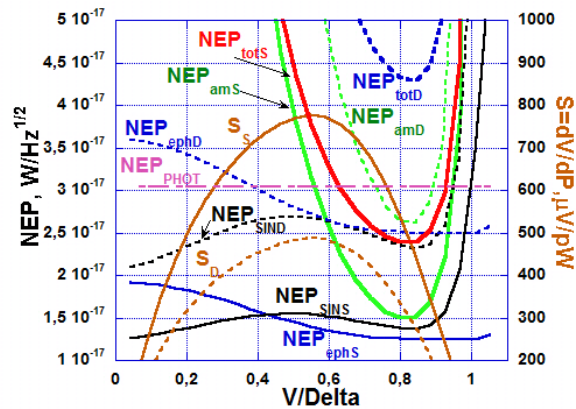


Figure 4 NEP components for the sparse rhombic array of bolometers.

Figure 4 presents NEP components for the sparse rhombic array of bolometers (marked by "S") and initial dense array of bolometers (marked by "D"). The sparse array consists of 2 CEBs in parallel ($W=2$) and 64 CEBs in series ($N=64$). Responsivity, S_v , is shown for both cases referred to the right axis. Parameters: $f=145$ GHz, $P_o = 2$ pW $I_{amp}=5$ fA/Hz^{1/2}. $V_{amp}=5$ nV/Hz^{1/2} (JFET), $R=6$ kOhm, $\Lambda = 0.01$ μm^{-3} , $T=300$ mK. RF design and analysis, numerical analysis are provided in 3.5.2 and 3.5.3, respectively.

4th chapter presents a concept of a millimeter and terahertz broadband generator based on a chain of capacitively coupled thermocouples forming a hybrid transmission line with an infinite phase velocity and excited by optical pulses from a femtosecond laser. A numerical

model of such a hybrid line is presented, as well as the results of numerical modeling of its dispersion characteristics in the range of 20-45 GHz. The simulation results are compared with the calculation within the framework of the equivalent UC scheme for lumped elements. An equivalent circuit is created for the transmission line and its properties are studied. We mentioned how it is possible to generate a terahertz wave using nonequilibrium states of an electron gas in metals. Thermocouples which are combined in a hybrid transmission line with superluminal phase velocity for their mutual synchronization. The experimental progress is processing to be practically tested and evaluated in subsequent work to expand the investigation.

4.1 An overview of left handed metamaterials is provided to better understand the **4.1.1** LH transmission line. With these two premises we open the topics of **4.2** Composite right / left handed transmission line. **4.2.1** Balanced and unbalanced Composite right / left handed transmission line are described and then in **4.3** nonequilibrium electrons in metals are discussed.

The total distribution of the electron gas $f(k)$ and phonons gas $g(q)$ are²⁰

$$\frac{\partial f(k)}{\partial t} = \frac{\partial f(k)}{\partial t} \Big|_{\text{el-el}} + \frac{\partial f(k)}{\partial t} \Big|_{\text{el-phon}} + \frac{\partial f(k)}{\partial t} \Big|_{\text{abs}} \quad (12)$$

$$\frac{\partial g(q)}{\partial t} = \frac{\partial g(q)}{\partial t} \Big|_{\text{phon-el}} \quad (13)$$

where k and q are the wave vectors of electrons and phonons, respectively. The components of the two equations described in **4.3.1**, **4.3.2**, **4.3.3** and **4.3.4** are discussed separately. **4.3.5** presents a new concept of the thermoelectric structure that generates microwave and terahertz signals when illuminated by femtosecond optical pulses. The structure consists of a series array of capacitively coupled thermocouples. The array acts as a hybrid type microwave transmission line with anomalous dispersion and phase velocity higher than the velocity of light. This allows for adding up the responses from all the thermocouples in phase. The array is easily integrable with microstrip transmission lines. Obtained dispersion curves from both the lumped network scheme and numerical simulations are presented. In **4.4** the transmission line model (Figure 5 illustrates two strips UC of this structure.) of this structure is analysed numerically and **4.5** is the summary of this chapter.

²⁰ Rethfeld B., Kaiser A., Vicanek M., Simon G. Ultrafast dynamics of nonequilibrium electrons in metals under femtosecond laser irradiation// Physical Review B. — 2002. — V. 65, № 21. — P. 214303.

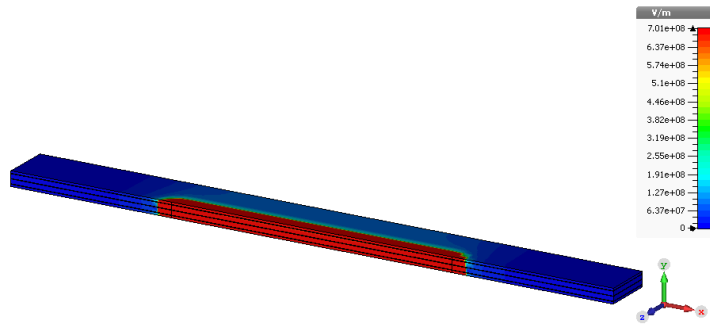


Figure 5 Extracted E- field distribution by the Eigenmode solver

5th chapter provides several plasmonic nano-structures for different applications. In **5.1** an attempt is made to explain the basic case of the drag electron effect and review designs which before are studied. **5.1.2** presents applications of surface plasmon photonics. Then **5.1.3** refers to the equation of motion for a better understanding of the concept of plasmonics, the drag effect and the drude model. **5.1.4** Summarizes Maxwell's equations for surface plasmon polaritons. **5.2** reports a numerical study of drag effect plasmonic metamaterial consisting of three layers SiO₂, Au, Si with the aim of absorption from 0.749 μm to 1.199 μm in spectral regime for infrared operation. An acceptable result from absorption by using the drag effect plasmonic metamaterial is obtained. **5.3** reports a numerical study of edge states plasmonic metamaterial consisting of four layers SiO₂, Ag, SiO₂, Si with the aim of molecules detection in visible spectral regime for near field Raman spectroscopy operation. Here, an acceptable result from edge modes by using the topological insulator is obtained. Two same array patterns of honeycomb lattices on the surface are connected together in a mirror-like manner. The structure design is presented in **5.3.2**, the results are in **5.3.3** and **5.3.4** is the summary of this subsection. In **5.4** a tunable plasmonic absorber composed of an elliptically grooved metallic film sandwiched between two dielectric layers is presented. To understand the optical response of the structure, its absorption spectrum and resonance modes profiles are numerically calculated using CST microwave studio. It is shown that the proposed device can provide two absorption peaks, in the near-infrared region, with absorption coefficients dependent upon the polarization angle of the incident light. Therefore, using a Faraday rotator and applying a variable external magnetic field, the device can be converted into a tunable magneto-optic modulator. From a different point of view, the proposed device is applicable as a sensor to measure mechanical rotations from 0 to 90 degrees. Besides, it is discussed that by adding a graphene layer to the structure, a tunable dual band modulator is realized, by which two absorption bands can be adjusted independently. Simulation results show that, modulation of absorption per graphene Fermi energy, about 73.33 %/eV and 69.54 %/eV are achieved for the first and the second peaks, respectively. After an introduction in

5.4.1 proposed structure and operating principle are discussed in 5.4.2. Figure 6 shows a schematic of this plasmonic nano-structure.

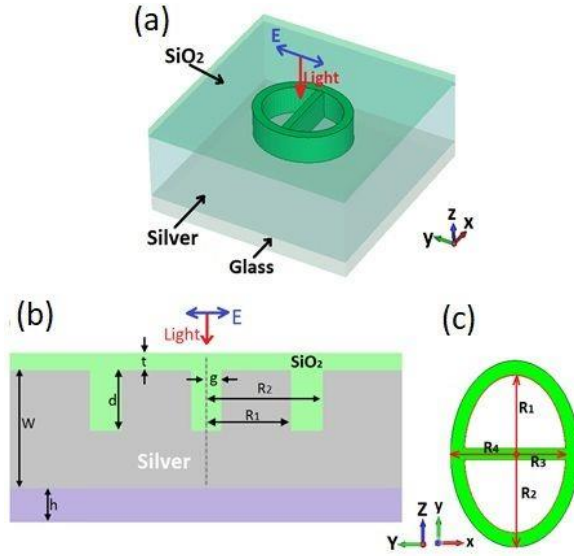


Figure 6 Schematic illustration of the proposed plasmonic absorber

Figure 6 is a schematic illustration of the proposed plasmonic absorber. Figure 6 a) is 3-D schematic of a UC; Figure 6 b) cross sectional view of a UC; and Figure 6 c) is the top view of the grooved ellipse with a major axis parallel to the y-axis. The array of the absorber is created by repeating the UC along the x and y directions with a period of $P= 1300$ nm. The initial polarization direction of the incident light is assumed to be parallel to the y-axis. The results of numerical simulation are in 5.4.3. It is mentioned that by add a layer of graphene to this structure two peaks can be tunable separately. μ_c is a factor for tunability by graphene layer according to Kubo equation²¹:

$$\sigma_g = \sigma_g^{inter} + \sigma_g^{intra} , \quad (14)$$

$$\sigma_{intra} = -j \frac{e^2 k_B T}{\pi \hbar^2 (\omega - j2\Gamma)} \left[\frac{\mu_c}{k_B T} + 2 \ln \left(\exp \left(-\frac{\mu_c}{k_B T} \right) + 1 \right) \right] \quad (15)$$

and

$$\sigma_{inter} = -j \frac{e^2}{4\pi \hbar} \ln \left[\frac{2|\mu_c| - \hbar(\omega - j2\Gamma)}{2|\mu_c| + \hbar(\omega - j2\Gamma)} \right] , \quad (16)$$

where σ_g^{inter} and σ_g^{intra} are originated from the inter-band and intra-band transitions, respectively. e , T , Γ , k_B and \hbar are the electron charge, temperature, the phenomenological scattering rate, the Boltzmann constant, and the reduced Planck constant, respectively. The chemical potential of graphene is represented by μ_c , which depends on the charge carrier density, and can be controlled by applying an external voltage. Equation 15 deals with the intra-band

²¹ Hanson G. W. Dyadic Green's functions and guided surface waves for a surface conductivity model of graphene// Journal of Applied Physics. — 2008. — V. 103. — P. 064302.

electro-photon scattering, and Equation 16 is the inter-band transition contribution, which is approximated for $\hbar\omega \gg k_B T$ and $|\mu_c| \gg k_B T$. We have chosen $T = 300$ K, $\mu_c = 0$ eV and $\tau = 0.3$ ps in our simulations, where $\tau = 1/2\Gamma$ is the relaxation time of electrons in graphene. Figure 7 shows the effect of lateral rotation of the polarization vector on the absorption spectrum. Figure 7 a) is the absorption spectrum for different polarization angles from 0 to 90 degrees. The inset shows the angle between the polarization vector (dashed blue vector) and the y-axis. Figure 7 b) is The electric field distribution of the structure at wavelength $\lambda_1 = 1520$ nm, while $\theta = 45^\circ$; Figure 7 c) is the electric field distribution of the structure at wavelength $\lambda_2 = 1720$ nm, while $\theta = 45^\circ$. **5.4.4** is the conclusion section. Figure 8 presents the absorption spectrum with and without graphene layer, the graphene chemical potential is 0 eV. The inset shows the alignment of the elliptical resonator. Figure 9 illustrates the absorption spectrum of a mono-layer graphene in vacuum for various Fermi energies, over the desired wavelength range. The wavelength at which the graphene absorption changes from 0 % to 2.3 % is the wavelength corresponding to the Fermi level in the graphene sheet.

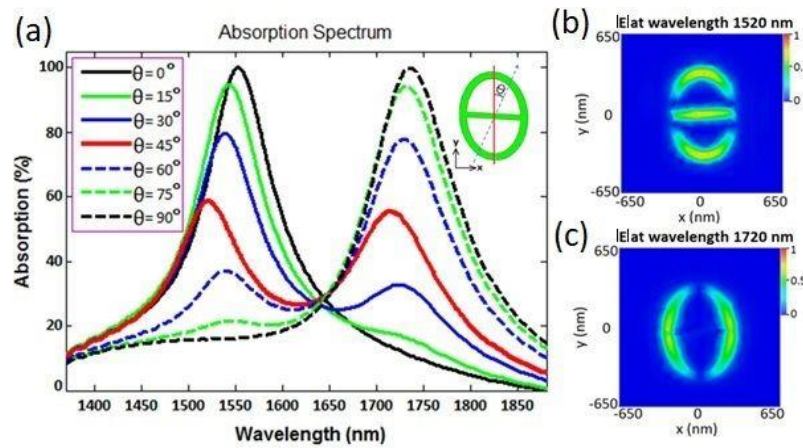


Figure 7 The effect of lateral rotation of the polarization vector on the absorption spectrum.

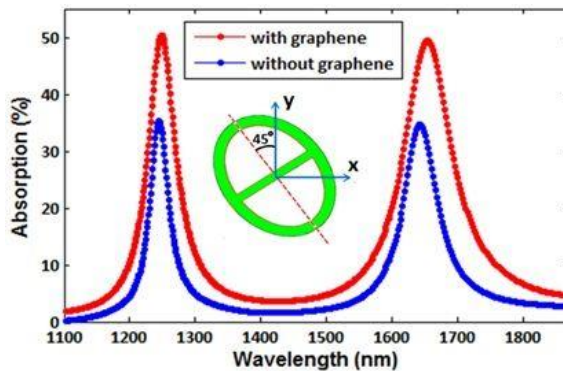


Figure 8 Absorption spectrum with and without graphene layer.

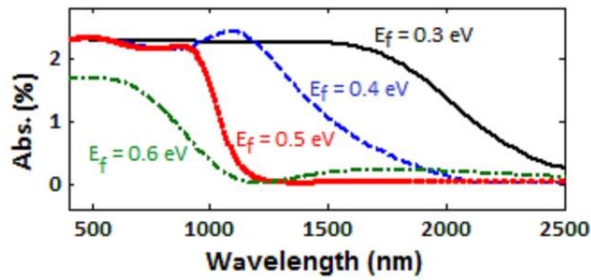


Figure 9 The absorption spectrum of a mono-layer graphene in vacuum for various Fermi energies, over the desired wavelength range.

In 5.5 a plasmonic absorber consisting of graphene and silica layers coated on a metal film with concentric-rings grooves is presented and numerically investigated. The proposed structure provides two absorption peaks at near-infrared region. The absorptivity of each peak can be tuned independently, by controlling the chemical potential of the graphene layer. Modulation of absorption per graphene Fermi energy about 85 %/eV and 51.25 %/eV can be obtained for the first and the second peaks, respectively. The Proposed structure and operating principle is presented in 5.5.1. Figure 10 shows the schematic illustration of the proposed plasmonic absorber. Figure 10 a) is three dimensional schematic; Figure 10 b) is cross sectional view of the UC; and Figure 10 c) is top view of the UC. The graphene layer is considered as a 2D material located on top of the structure. The array of the absorber is created by repeating the UC along the x and y directions, with a period of $P=800$ nm.

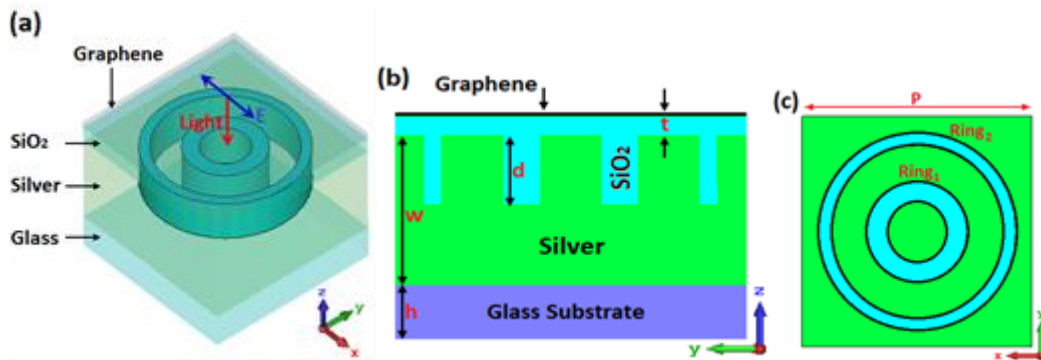


Figure 10 Schematic illustration of the proposed plasmonic absorber.

In 5.5.2 the simulation method is described. The proposed device is numerically modeled using a frequency domain solver by CST Microwave Studio. In the simulations, a UC boundary conditions in x and y directions are selected, and open boundary conditions along the z-direction are applied. The UC is illuminated by a normally incident plane wave with electric field parallel to the y-axis. Results are presented in 5.5.3.

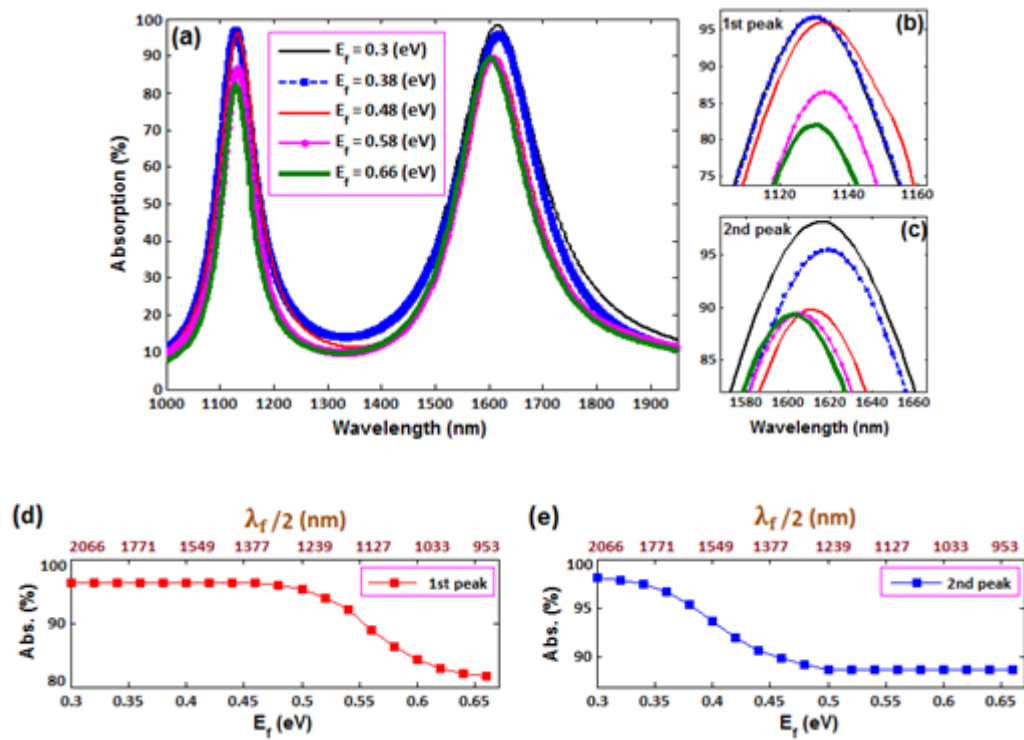


Figure 11 The influence of changes of the chemical potential on the optical response of the device.

Figure 11 is the influence of changes of the chemical potential on the optical response of the device. Figure 11 a) is absorption spectrum of the proposed structure for different Fermi energies of the graphene layer; Figure 11 b,c) are the absorption spectrum of the peaks under the variation of Fermi energy of the graphene layer; Figure 11 d,e) are the variations of the absorption magnitude of two modes as a function of graphene Fermi energy at resonance wavelengths of 1125 nm and 1615 nm. **5.5.4** is the conclusion of **5.5**.

Author’s publications on the dissertation topic

1. **Beiranvand B.**, Sobolev A. S. A proposal for a multi-functional tunable dual-band plasmonic absorber consisting of a periodic array of elliptical groove// Journal of optics. — 2020. —V. 22, № 10. —P. 105005. DOI: <https://doi.org/10.1088/2040-8986/abb2f3>
2. Sobolev A. S., Kuzmin L. S., **Beiranvand B.**, Kudryashov A. V., Ilin A. Ultrawideband Metamaterial-Based Array of Cold-Electron Bolometers// Radiation and Scattering of Electromagnetic Waves (IEEE). —2019. —P. 196-199. DOI: [10.1109/RSEMW.2019.8792785](https://doi.org/10.1109/RSEMW.2019.8792785)

3. Sobolev A. S., **Beiranvand B.**, Chekushkin A. M., Kudryashov A. V., Tarasov M. A., Yusupov R. A., Gunbina A., Vdovin V. F., Edelman V. Wideband metamaterial-based array of SINIS bolometers// European Physical Journal Web of Conferences (EDP Sciences).—2018.—V.195. —P. 05009. DOI: [10.1051/epjconf/201819505009](https://doi.org/10.1051/epjconf/201819505009)
4. Kuzmin L. S., Sobolev A. S., **Beiranvand B.** Wideband Double-Polarized Array of Cold-Electron Bolometers for OLIMPO Balloon Telescope// Transactions on Antennas and Propagation (IEEE). —2020. DOI: [10.1109/TAP.2020.3026874](https://doi.org/10.1109/TAP.2020.3026874)
5. **Beiranvand B.**, Sobolev A. S., Sheikha A. A proposal for a dual-band tunable plasmonic absorber using concentric-rings resonators and mono-layer graphene// Optik International Journal for Light and Electron. —2020. —V. 223. —P. 165587. DOI: <https://doi.org/10.1016/j.ijleo.2020.165587>
6. Бейранванд Б., Соболев А. С. Гибридная линия передач с интегрированной цепочкой термопар для генерации терагерцового излучения// Труды 60-й Всероссийской научной конференции МФТИ. —2017. —с. 149-151.
7. Бейранванд Б., Вдовин В. Ф., Гунбина А. А., Ермаков А. Б., Лемзяков С. А., Мансфельд М. А., Махашабде С., Нагирная Д. В., Соболев А. С., Тарасов М. А., Фоминский М. Ю., Чекушкин А. М., Эдельман В. С., Юсупов Р. А., Якопов Г. В. Матрицы планарных антенн с интегрированными СИНИС болометрами для радиоастрономических исследований// Сборник трудов VI Всероссийской микроволновой конференции. —2018. — с. 253-257.
8. Соболев А. С., Бейранванд Б., Тарасов М. А., Юсупов Р. А., Гунбина А. А., Чекушкин А. М., Эдельман В. С. Двухчастотная метаповерхность с интегрированными СИНИС болометрами// Сборник трудов VI Всероссийской микроволновой конференции. —2018. —с. 310.
9. Бейранванд Б., Соболев А. С., Кудряшов А. В. Гибридная линия передач с интегрированной цепочкой термопар для генерации терагерцового излучения // Труды МФТИ. —2020. —Т. 12, № 3. —с. 87–93.